COMPARISON OF WAVELET ANALYSES APPLIED TO VERY ROUGH BOUNDARY LAYER DATA

Kellnerová, Radka

Kukačka, Libor

Odin, Julie

Uruba, Václav

他

出版情報：COE Lecture Note. 36, pp.36-45, 2012-01-27. 九州大学マス・フォア・インダストリ研究所
バージョン：
権利関係：

Proceedings of the Czech–Japanese Seminar in Applied Mathematics 2010
Czech Technical University in Prague, August 30 - September 4, 2010
pp. 36–45

COMPARISON OF WAVELET ANALYSES APPLIED TO VERY ROUGH BOUNDARY LAYER DATA

RADKA KELLNEROVÁ LIBOR KUKAČKA JULIE ODIN
VÁCLAV URUBA PAVEL ANTOŠ ZBYNĚK JAŇOUR

Abstract. Wavelet analysis is tested using the data from a simulation of turbulent atmospheric boundary performed in a wind channel. Model of urban streets is positioned on the test section floor. The large size of the model has led to high value of the roughness. Experiment involves hot-wire (HWA) and time-resolved Particle Image Velocimetry (TR-PIV) measurements inside the street canyon. Wavelet analysis applied to the velocity data results in information about frequency spectrum and temporal location of energetic harmonic structures in the flow field. Comparison of the HWA results with those obtained by PIV has shown agreement of spectral characteristics, confirming the legacy of their application. Total power spectra from different position in the street canyon were analysed and mutually confronted.

Key words. wind-channel, Wavelet analysis, HWA, PIV, street canyon.

1. Introduction. Wavelet analysis was introduced by Morlet in 80's, originally to processing of seismic signals. Since that time this mathematical technique underwent a rapid evolution and especially due to Farge [1] became applicable on experimental data. With a fast development of signal processing in wind-tunnel experiments, wavelet analysis begun to be extensively employed on pressure and velocity data (Gao [3], Feigenwinter [2], Xia [13], Watanabe [12], Huang [5]). However, the exact interpretation of its conclusions is still difficult, mainly because it sometimes produces fuzzy and blurry results with no transparent physical meaning. In this paper we have focused on testing alternative wavelet functions and afterwards, on decoding the physical meaning of the obtained local power spectra in the flow.

2. Experimental set-up. The atmospheric boundary layer above a very rough terrain was simulated in a wind channel with series of identical, mutually parallel street canyons on the test section floor (see Figure 2.1 - upper). These generated a highly turbulent flow. Intensity of turbulence reached the values up to 40%. Reference velocity at the nozzle exit was 5 m/s.

The test section dimensions were 0.25 m × 0.25 m in cross-section and about 3 m in the longitudinal direction. The area of interest was as far downstream as possible, behind the 20th row from the test section entrance, in order to obtain the turbulent boundary layer there to be fully developed (see Figure 2.1). For verification purposes, the mean longitudinal velocity profile in the investigated position and in other three surrounding positions were measured by Pitot probe. The deviation between the profiles did not exceed 1.5%.

Two geometries of model building roofs were used - the triangular and flat shapes as shown in Figure 2.2. The model was manufactured in the scale of 1:400. This means the 20m high buildings were modeled by 50 mm high objects. The street aspect ratio equaled to one, what corresponded to the classical conditions in research.

[1]Department of Meteorology and Environment Protection, Faculty of Mathematics and Physics, Charles University, Prague, Czech Republic.
[2]Institute of Thermomechanics, AS CR, Prague, Czech Republic.

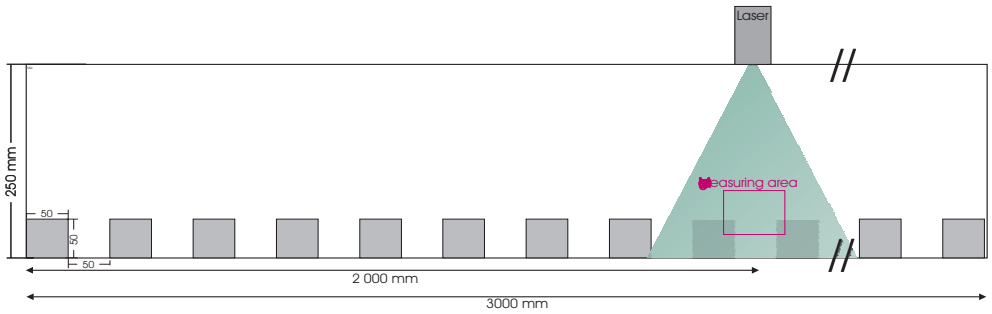

FIG. 2.1. *Scheme of model of street canyons inside the channel. Flow is coming from the left side. Green area denotes the sheet light of laser for PIV.*

According to Oke [9], this aspect ratio belongs to so-called skimming regime, where the turbulent fluctuations dominate over the time-averaged flow, as also concluded Louka [8].

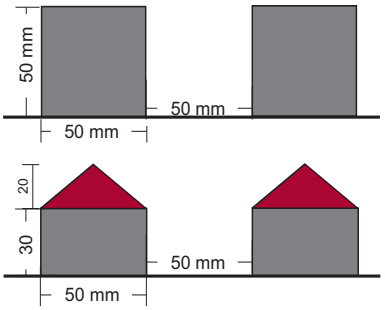

FIG. 2.2. *Scheme of buildings with flat roof (upper) and pitched roof (lower).*

In the first measurement series we have used CTA hot-wire anemometry. The HWA probe was gold-plated Dantec 55 P01, with dimension of 5 m × 1.25 mm. This probe is able to measure longitudinal velocity component with sampling frequency 25 kHz. Acquisition time at each spatial position was 30 s, which produced one data series with 750,000 values.

In the next series, we have used Particle Image Velocimetry of high repetition rate (500 Hz). This produced a number of 2-D snapshots of vectors of instantaneous velocity. The wind tunnel was filled by oil droplets (Dantec Fog Fluid) of mean radius 1 μm. Thanks to the high level of turbulent intensity the droplets were evenly distributed over the whole test section, producing images of high quality. Raw PIV data were then processed by the software DynamicStudio v. 3.00. One run of PIV measurement consists of 1600 snapshots, each of them with more than 4800 velocity vectors. In the table 2 below, the parameters of PIV set-up are presented.

3. Results.

3.1. Local power spectrum. Wavelet analysis applied to the data series of some physical property reveals the frequency and time of its appearance present in the signal. The original measured quantity might be arbitrary, however it is mostly velocity, pressure, temperature, or humidity. The basic principle of wavelet transformation is finding the best convolution between signal and the so-called mother wavelet.

Table 2	Diode pumped Nd:YLF laser
Repetition rate	500 -1000 Hz
Repetition rate	1280 × 1024 pxs
Interrogation area	32 × 32 pxs
Overlapping	50% (80 × 64 vectors)
Energy	10 mJ
Area	100 × 100 mm
Acquisition time	3.2 s

The mother wavelet function might be arbitrary function that fulfills a criterion of admissibility, which means that the function quickly falls to zero with $f \to \pm\infty$ and it has a zero mean value. We have tested two commonly used mother functions, known as "Mexican hat" and "Morlet function". Definition of these functions is presented in the table 3.1 below.

Table 3.1	Wavelet mother function
Mexican hat	$\psi(t) = (1 - t^2)e^{t^2/2}$
Morlet	$\psi(t) = \pi^{-1/4} e^{i2\pi f_0 t} e^{-t^2/2}$

The Mexican hat (Figure 3.1 - left) is popular for its good ability to 'feel' the so-called ramp-like patterns in the flow. These patterns were detected by in-situ measurements above plant canopy and are associated with a small local microfront (Shaw and Finnigan [10]). The term microfront here represents a dynamic event of a velocity convergence together with a production of sharp gradient of scalar quantity (temperature, humidity, pressure), observed at several levels inside the flow.

Morlet function (Figure 3.1 - right) contains more waves and it is therefore more sensitive to a sinusoidal signal character. It has also simpler image in the Fourier space which results in better localisation of frequency. Furthermore, Morlet function is complex, so that the real and imaginary parts may be diagnosed separately. The phase can be extracted as well. Since the spectrum algorithm starts from velocity fluctuations of the original time-series, the square of the modulus of the wavelet coefficient represents turbulent kinetic energy. In this study, the power, i.e. the square of the modulus divided by acquisition time, was evaluated since it brings a useful information about highly energetic harmonic structures.

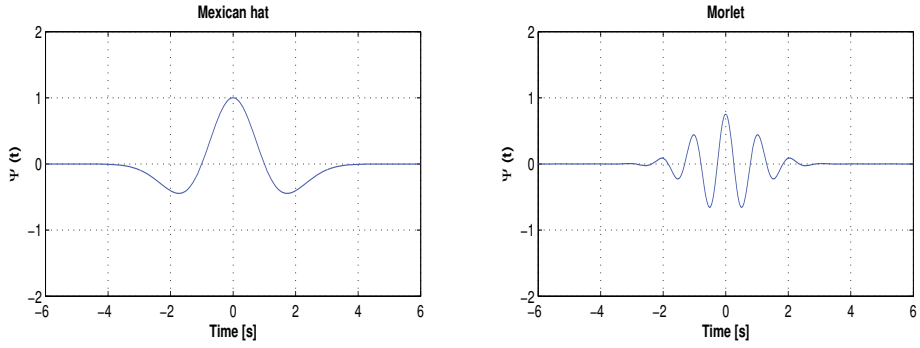

FIG. 3.1. *Left: Function called Mexican hat (after its shape). Right: Function called Morlet, characteristic angular frequency* $\omega_0 = 6$. *Both depicted in time-domain.*

For calculation, we adopted Matlab code developed by Torrence & Compo [10], modified after the recommendation of Ge [4] and properly normalised. Since normalisation varies from author to author, we introduced the normalisation by fitting of wavelet total power spectrum on previously verified Fourier power spectrum (Figure 3.2). The black solid line is theoretical curve proposed by Karman. This curve is derived from the measurements inside the atmospheric boundary layer (Kaimal & Finnigan [6]).

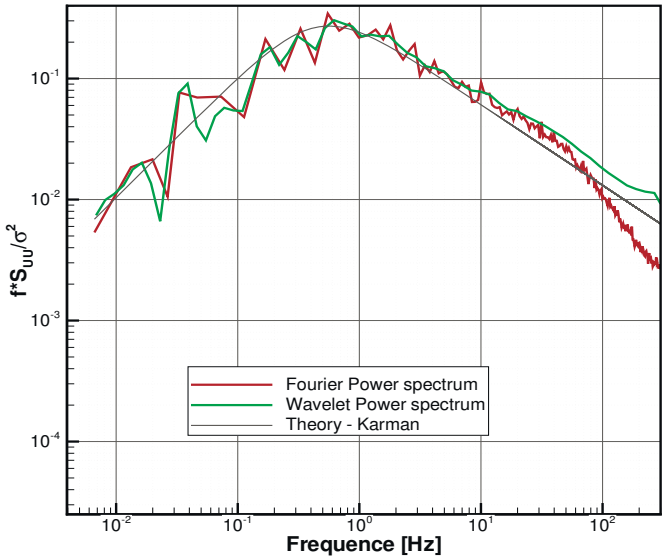

FIG. 3.2. *Comparison between Fourier and Wavelet spectrum for normalisation purpose.*

We have tested both alternative functions and compared their local power spectra. In Figure 3.3 - upper is seen the original signal, a simple sine with frequency of 3 and 5 Hz during the first and the second half-period, respectively. Left part of the lower picture depicts transformation into local power spectra by Morlet function, whereas right part of the lower picture displays the wavelet transformation with Mexican hat function. On the abscissa is plotted time in second, on the ordinate axis is plotted frequency in Herz.

The Morlet power pattern is apparently smoother, better defined in frequency, and more compact than the one derived from the Mexican hat function. Notwithstanding, the magnitudes of power reach the same values for both functions. Furthermore, the total spectral characteristics collapse into each other (not shown). For the very first introduction into the Wavelet analysis, we found Morlet mother wavelet to be more suitable. Henceforward, all Wavelet analyses mentioned in this paper were performed with the Morlet function.

Regarding the interpretation, authors usually obtain frequency and time information of a highly energetic event, because it is clear from the scalogram *when* 'it happens' and *what frequency* 'it happens' *with*. Thus, one could get a deeper understanding about particular frequencies appearing in the flow and the time of their emergence - or perhaps duration of the events.

Nevertheless, the shapes of particular power patterns are often blurry, very individual and lacking any united repetitive geometry across the scalogram. It is therefore

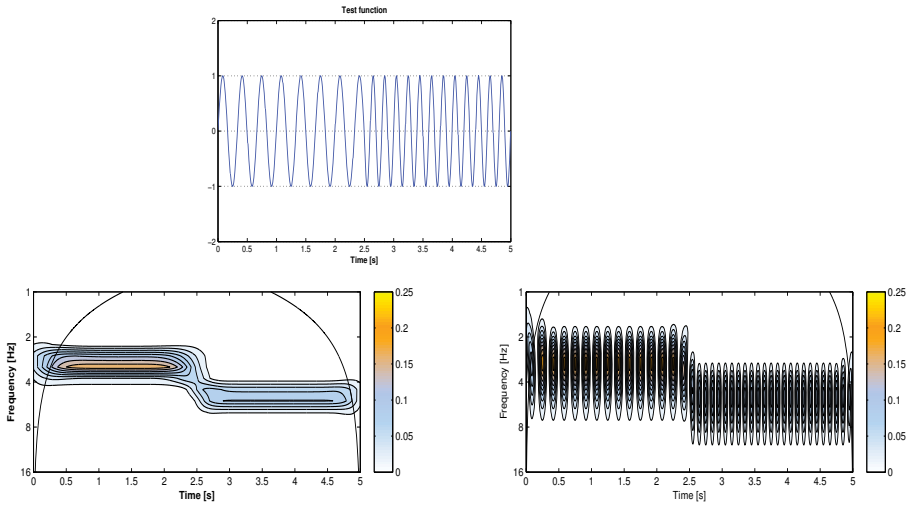

FIG. 3.3. *Power spectra for the test signal with two consecutive frequencies of 3 and 5 Hz (upper). Morlet function (left) produces smooth solid pattern, whereas Mexican hat (right) brings number of separated regions with maximum energy laid in the same frequency.*

difficult to understand the meaning of the detected events. An example is seen in Figure 3.4. Therefore we carefully compared scalograms with series of snapshots recorded during PIV measurement. Then we attempted to establish a link between the spots in the scalogram and the vector field in the snapshots.

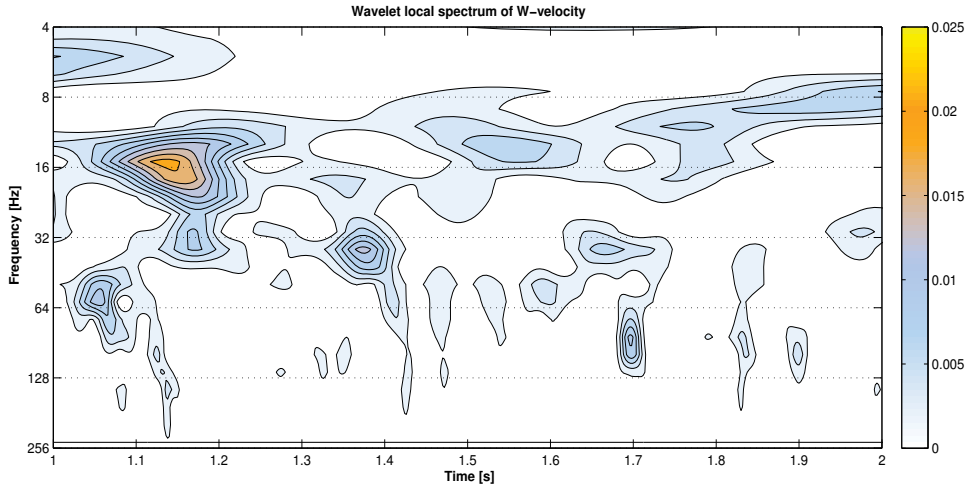

FIG. 3.4. *Example of local wavelet analysis of vertical velocity component at level $Z/H = 1.2$, where H denotes a height of the building. Black solid line is Cone of influence, above which the spectrum values are incorrect.*

Magnitude of the power in scalogram depends on a progression of velocity with time. The more energetic is the structure from turbulent kinetic energy point of view and the more is the harmonic history of its fluctuations, the larger magnitude

of wavelet coefficient is obtained in the scalogram. According to this, the highest coefficient level are often given to the consecutive series of large eddies, since they supply velocity field by large quasi-harmonic variations. For example, tiny and constant equidistant separation between the eddies leads to both better convolution with the Morlet function and to higher energetic contribution.

A demonstrative example is captured in the Figure 3.5 - left. The before-mentioned vortices passed so quickly that the detection of sinusoidal waves are on the very edge of temporal-resolution of PIV system (500 Hz). Three vortices crossed over the analysed position (red dot in the Figure 3.5 - right) and imprinted themselves as triple consecutive sines functions. Entering of the vortex is recognisable by the negative vertical fluctuation, which means that a sweep event in the front of eddy touches this position. Then the positive vertical fluctuation announces that the vortex passed across and ejection event on the rear part comes into this place. A street canyon surrounded by buildings with pitched roof is shown there filled by vectors of instantaneous velocity (Figure 3.5 - right). Snapshot catches the situation where the analysed position is just in a saddle point between the first and the second vortex, marked by red circles.

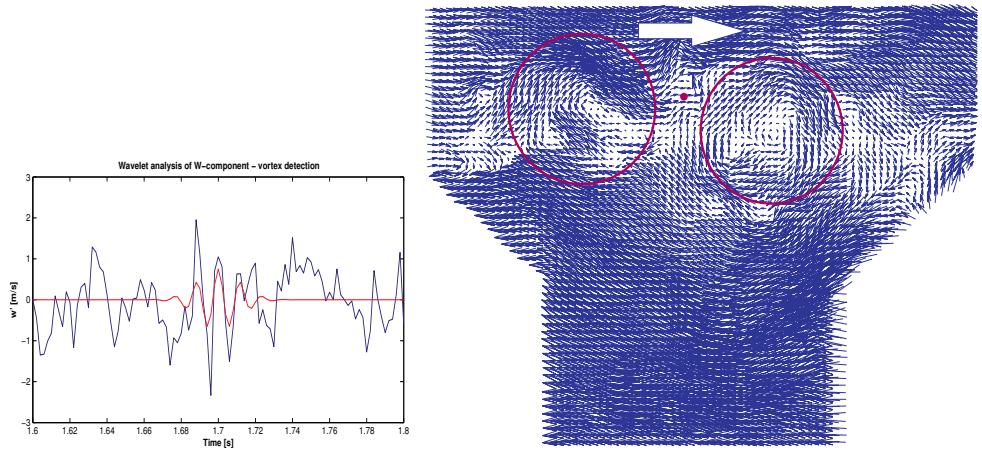

FIG. 3.5. *Left: Example of good approximation of signal by the Morlet function. Right: Two red circles mark the two consecutive vortices in the vector field between buildings with pitched roof.*

The before-mentioned event is captured in the wavelet local spectrum for vertical velocity component as the vertically elongated oval at the time t=1.7 s, with frequency around 84 Hz (see Figure 3.4). Such a pattern witnesses a passage of one vortex or series of vortices.

The nearly horizontal orange coloured spot at the time t=1.15 s, with frequency around 16 Hz, is an evidence of a strong vertical motion - such as sweep or ejection. Especially, when the sweep and the ejection alternate one by one with the corresponding frequency. Instantaneous velocity field reflecting this event is seen in the Figure 3.6. The red rectangle marks a strong sweep event crossing the investigated position. To conclude, the horizontally prolonged blurs reflect a long-term oscillation at a certain frequency. Therefore, the blurs mean the passage of significant sweep and ejection event.

Comparison between HWA and PIV technique from wavelet analysis point of view was also performed. It is important to emphasize that the original signals from HWA and PIV technique are taken in the same position, but from practical reasons,

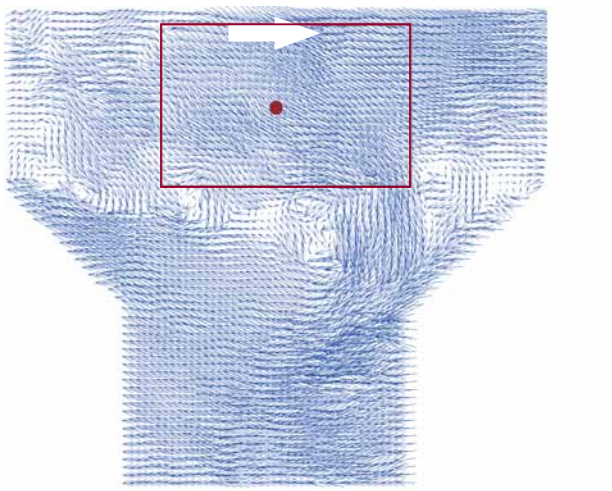

FIG. 3.6. *Sweep event (red rectangle) passing measuring position (red dot) in vector field taken from PIV records.*

not in the same instant of time. They were measured one after another. Despite the different sampling frequencies, the signals do not deviate from each other in statistical point of view. For example, considering typical statistics like mean velocity, standard deviation, skewness and kurtosis, the total deviation between HWA and PIV values is less the 4.5%.

Nevertheless, there was a distinction in the post-processing. HWA data are simply derived from the original voltage signal by the formula achieved in the previous calibration. On the other hand, the PIV measurement requires more complex processing. Commercial software for PIV (DynamicStudio v. 3.00) is able to post-process images, create vectors of velocity and reject possible spurious vectors. At the very beginning, we applied adaptive correlation to each ensemble from one measurement run. The adaptive correlation is actually the spatial correlation in each interrogation area. It allows to evaluate a preliminary vector field. Thereafter, a range validation was used to filter out the most striking spurious vectors and a moving average validation could replace them by a reasonable estimate.

Thus these distinct ways might result in dissimilar wavelet scalograms (Figure 3.7). Since the power spectrum is normalised by the acquisition time and these times instants deviate for both methods, the magnitude of power is not the same. However, the maximum energy belongs to the same frequency range for both data sources (Figure 3.8 - left). Finally, the high similarity of total power spectrum (see below) confirmed applicability of both measuring devices in very turbulent flow.

3.2. Total power spectrum. Total power spectra are an integral sum of local power spectra over time. Since the HWA provides very high sample frequency of 25 kHz, the spectral characteristics can describe the energy density even up to the Nyquist frequency of 12.5 kHz. Comparison between HWA and PIV data was made for several altitudes above the canyon (see Figure 3.8 - left). Wavelet spectrum for HWA data is more smooth because the finest step of *scale in the Wavelet transformation* is $2 * dt = 8.10^{-5}$, where dt is time step. The finest PIV *scale* resolution is 'only' $2 * dt = 4.10^{-3}$ what results in poorer frequency resolution. HWA spectrum includes

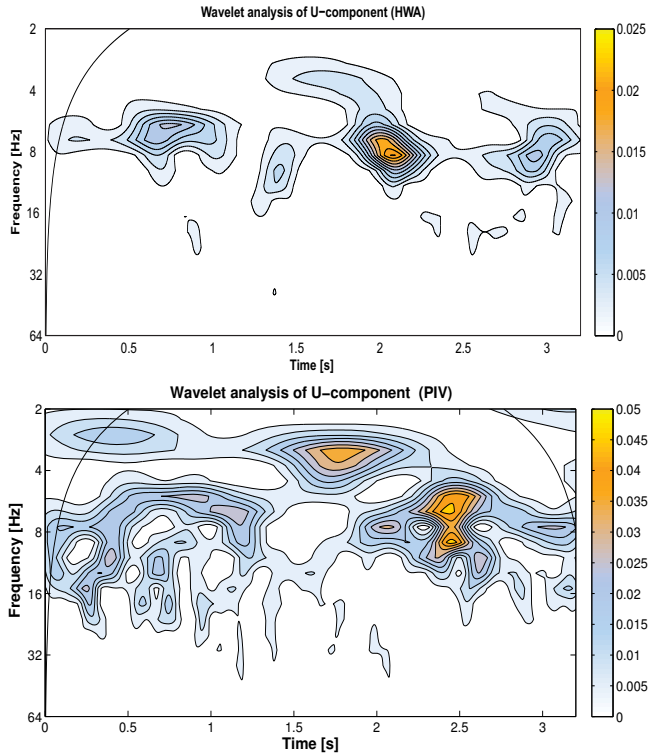

FIG. 3.7. *Upper: Local wavelet power spectra applied on PIV velocity data - data rate of 500 Hz (left). Lower: Velocity in the same position is measured by HWA - data rate of 25 kHz, and analysed by the same method.*

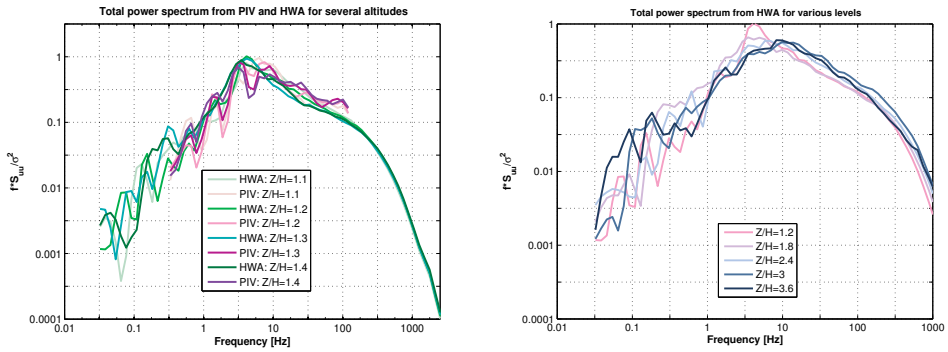

FIG. 3.8. *Left: Total power spectrum derived from HWA and PIV velocity series for several altitudes Z/H=1.1-1.4. Right: Total power spectrum derived from HWA velocity series for several altitudes Z/H=1.2-3.6.*

explicit peaks around 5 Hz velocity signal at the lowest level Z/H=1.2, where H denotes the height of the building. At the higher level Z/H=3, the peaks is around 14 Hz - see Figure 3.8 - right.

Inside the street canyon, the number of spatial positions were analysed and their energy spectra were evaluated. Figure 3.9 - left shows the example of a total wavelet

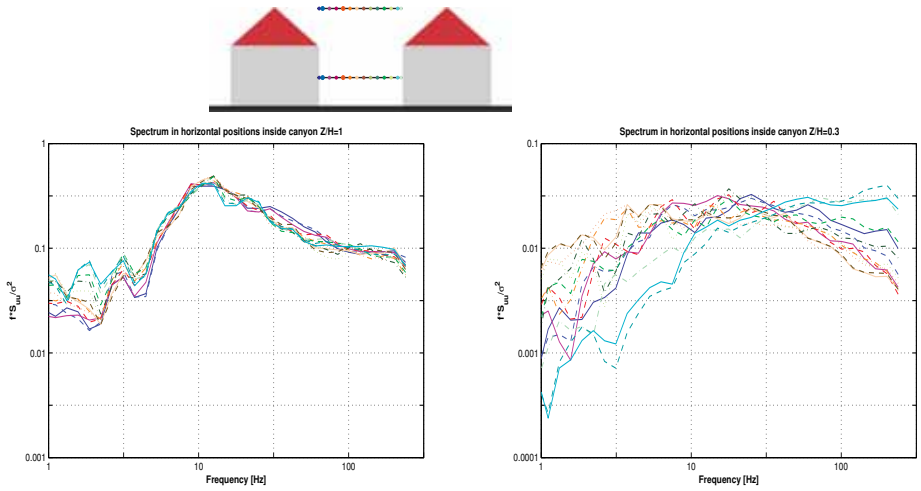

FIG. 3.9. *Left: Total power spectrum in several for spatial positions at altitude Z/H=1. Right: Total power spectrum at altitude Z/H=0.3 (check colourful scheme on the top).*

power spectra at the roof-top level (Z/H=1) location, where the profiles collapse well into one another. A common peak at around 10 Hz can be seen for all horizontal positions. Regarding the low frequencies around 1 Hz, the larger eddies or wavy events reach more often the windward region. It is because the eddies get disturbed and broken on the sharp edge of leeward roof. Thus the energy of big eddies (low frequencies) is slightly lower on the leeward side. However, it should be taken into account that the events with frequency of 1 Hz cannot appear often in the recording with only 3.2 s of duration. Thus, the statistical description of these low-frequency dynamics is insecure.

Figure 3.9 - right reflects the situation lower, inside the canyon. The plot shows the significant variability of spectra in canyon. This happens due to markedly different flow regimes on the leeward and windward side.

4. Conclusion. Experiment with very turbulent flow in the wind-channel was performed. Velocity time-series from HWA and planar vector fields recorded by PIV were obtained. The Wavelet analysis was applied to data using two popular alternative types of mother functions. Due to the better image in Fourier space, Morlet function was chosen as the more suitable one for the present analysis of the very turbulent type of flow within an urban area. Particular spots in the local power spectrum were checked together with PIV recordings in order to reveal physical interpretation of spectral power patterns. The circular spots at high frequency represent vortices, which cross along the measurement position in consecutive way. The 'ameboid' shapes of the spots at lower frequency is non-recurring sweep or ejection situations. Horizontally elongated patterns depict the passage of multiple sweep and ejection events in quasi-periodic situation.

Total spectra from both measuring methods collapse well into each other. We have checked also various spectra from various spatial positions inside the canyon. The positions in the lower part of canyon exhibit a significant deviation. The flow regime is very complex inside street and depends very much on the particular location. At the roof-top level and above the canyon, the spectra collapse much better, with

only a minor differences observed on the leeward side.

Acknowledgment. Authors kindly thank for support by GAUK No. 136609 (115-10/259266). The experiment could be performed at Institute of Thermomechanics with agreement and support by AV0Z20760514.

REFERENCES

[1] M. Farge, *Wavelet transforms and theit applications to turbulence*, Annual Reviews Fluid Mech. (1992), **24**, p. 395-457.

[2] C. Feigenwinter, R. Vogt, *Detection and analysis of coherent structures in urban turulence*, Theor. Appl. Climatol. (2005), **81**, p. 219-230.

[3] W. Gao, B. L. Li, *Wavelet Analysis of Coherent Structures at the Atmosphere-Forest Interface*. J. Appl. Meteor. (1993), **32**, p. 1717-1725.

[4] Z. Ge, *Significance Tests for the Wavelet Power and the Wavelet Power Spectrum*, Annales Geophysicae (2007), **25**, p. 2259-2269.

[5] Z. C. Huang, H. H. Hwung, K.-A. Chang, *Wavelet-based vortical structure detection and length scale estimate for laboratory spilling waves*, Coastal Engineering (2010), **57**, p. 795-811.

[6] J. C. Kaimal, J. J. Finnigan, *Atmospheric boundary layer flows: their structure and measurement*, Oxford University Press (1994).

[7] R. Kellnerova, L. Kukacka, V. Uruba, P. Antos, J. Odin, Z. Janour , *Wavelet and POD Analysis of Turbulent Flow Within Street Canyon*, Experimental Fluid Mechanics (2010), Conference proceeding, p. 263-270.

[8] P. Louka, S. E. Belcher, R. G. Harrison, *Coupling between air flow in streets and the well-developed boundary layer aloft*. Atmospheric Environment, (2000), **34**, p. 2613-2621.

[9] T. R. Oke, *Boundary Layer Climates*. Routledge, London, (1987).

[10] R. H. Shaw , J. J. Finnigan, *Eddy Structure Near Plant Canopy Interface. 17th Sym- posium on Boundary Layers and Turbulence*, San Diego, Canada, Conference proceeding (2006), p. J2.1.

[11] C. Torrence , G. P. Compo, *A Practical Guide to Wavelet Analysis*, em Bull. Am. Meteorol. Soc. (1998), **79**, p. 61-78.

[12] T. Watanabe, *LES Study on the Structure of Coherent Eddies Inducing Predominant Perturbations in Velocities in the Roughness Sublayer over Plant Canopies*, Journal of the Meteorological Society of Japan (2009), **87**, No. 1, p. 39-56.

[13] Z. Y. Xia, Y. Tian, N. Jiang, *Wavelet Spectrum Analysis on Energy Transfer of Multi-Scale Structures in Wall Turbulence*. Applied Mathematics and Mechanics -English Edition (2009), **30 (4)**, p. 435-443.